

# Forming limit of hot-rolled high-strength steels considering sheet thickness effect

Shi-Hong Zhang<sup>1\*</sup>, Wei-Jin Chen<sup>1,2</sup>, Shuai-Feng Chen<sup>1</sup>, Hong-Wu Song<sup>1</sup>, Si-Ying Deng<sup>1</sup>

<sup>1</sup>Shi-Changxu Innovation Center for Advanced Materials, Institute of Metal Research, Chinese Academy of Sciences, 110016 Shenyang,

<sup>2</sup>China Research Institute, Baoshan Iron and Steel Co., Ltd., 201999 Shanghai, China

**Abstract.** The forming limit curve (FLC) has been commonly used tool to predict the metal forming cracking in engineering. Whereas, based on the assumption of plane stress state, the formability prediction of thick sheet of hot-rolled high-strength steels is quite different from the experimental measurement. Finite element simulation was used to study the effect of sheet thickness. It is found that extra stress along thickness is introduced between inside and outside the instability region, which become larger increased. Additionally, the visco-plastic self-consistent (VPSC) model and the M-K model are combined to establish the VPSC-MK model for investigating the influence of thickness difference. With reasonable capture of thickness stress, accurate prediction of FLC under different sheet thickness of hot rolled high-strength steel (HR-HSS) is well realized via VPSC-MK model. That is, it is revealed that the sheet thickness effect for HR-HSS mainly origins from normal stress induced during necking process.

## 1 Introduction

In the automotive industry, hot-rolled high strength steels (HR-HSS) are employed widely in chassis parts of passenger cars and commercial vehicles, which can effectively reduce automotive weight for energy saving and emission reduction of carbon dioxide [1,2]. Due to trade-off between strength and ductility for metallic materials, their formability always decrease. Generally, trial and error iterations for profile design and forming process are always needed to produce complex component with HSS sheet [3]. Thus, accurate evaluation of the hot-rolled sheet formability is essential for improving design efficiency and quality of complex component.

For prediction of FCL for HR-HSS sheets with large thickness range (1.5~8.0 mm), a notable challenge is that their formability show close dependence on sheet thickness. To quantify the effect of sheet thickness, Assempour et al. [4] set the thickness stress as a ratio of the principal stress and substitute it into the M-K model for reasonably calculating the forming limit of AA6011 and STKM-11A sheets. Zhang et al. [5] predicted the forming limit of AA6111-T43 sheet by introducing the thickness stress into the M-K model as the ratio of the yield strength. A higher thickness compressive stress value makes a better forming

---

\*Corresponding author: [shzhagn@imr.ac.cn](mailto:shzhagn@imr.ac.cn)

performance. Meanwhile, the thickness stress can also be generated during bending of the sheet when the FLC is tested with a spherical punch [6]. Wang et al. [7] consider the thickness stress induced during Nakazima test and in-plane shear stress under friction via the modified M-K model to predict the formability of the sheet metal. The prediction accuracy of the modified model considering the thickness stress and friction stress is higher. However, the influence of thickness stress on forming limit was mainly investigated in the view of macroscopic constitutive model, while its influence mechanism needs to be further clarified. Additionally, systematically study for influence of thickness on formability is needed to improve the prediction accuracy of forming limit of hot rolled high strength steel.

In this study, the thickness effect and prediction model of forming limit of HR-HSS are studied. The VPSC-MK model coupled with the visco-plastic self-consistent model (VPSC) and the M-K model was established. By introducing the strain-path dependent thickness stress into VPSC-MK, accurate prediction of the forming limit of HR-HSS is achieved.

## 2 Experiments and methods

### 2.1 Experiments

S700MC was selected as a typical kind of HR-HSS sheet to study the mechanical behaviour and formability. According to ISO 6892-1:2019, the mechanical properties of the material were tested by using 100 kN Instron machine. The tensile speed was 1.5 mm/min, and two transverse and longitudinal extensometers were used to track the transverse and longitudinal tensile strains respectively. The plate-like tensile specimens were stretched along rolling direction. The parallel segment width of the sample was 20 mm, the scale distance was 80 mm, and each experiment was repeated twice. Additionally, Nakazima experiments were performed on a 750 KN Interlaken forming tester to obtain the material forming limits according to ISO 12004-2:2008. In order to reduce the effect of friction between the sample and the die on the experiment and make the fracture position as close as possible to the tip position, the teflon film and glycerin were used for lubrication

Note that, all the tests for mechanical property and formability of S700MC sheet were carried out under two thickness of 2.5 mm and 4.0 mm. In order to avoid the differences in microstructure feature and texture types between different batches, the S700MC steel with 4.0mm thickness is thinned to 2.5mm by the grinder.

#### 2.1.1 Finite element simulation

Fig. 1 shows the finite element model of uniaxial tensile specimen, on which points 1-6 are chosen for strain analysis. The maximum strain of tensile sample is set as point 1. Points 2, 3 and 4 are taken at each 3 mm along the tension direction, while points 5 and 6 are taken every 6 mm. The strain data of uniaxial tensile samples are obtained by FEM simulation. The diffuse necking strain is determined with principal strain difference between point 1 and point 6 larger than zero. While, the local necking strain is given as the ratio of the principal strain increment between point 1 and point 2 becomes larger than 20.

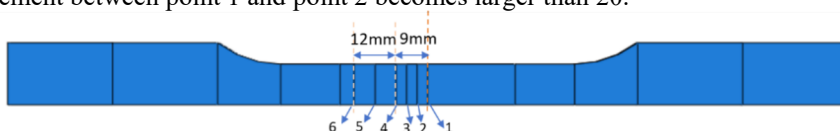


**Fig. 1.** The points chosen for strain analysis on the specimen for uniaxial tensile test

### 2.1.2 VPSC-MK coupled model

For the plastic deformation of single grain, certain slip system  $s$  can be initiated as resolved shear stress increase to the critical resolved shear stress. Thus, the strength of the material will increase with deformation continuing, that is, strain hardening will occur. In the VPSC model, the hardening equation adopts Voce hardening law, which can be expressed as

$$\tau_{crit}^s = \tau_0 + (\tau_1 + \theta_1 \Gamma) \left\{ 1 - \exp\left(-\frac{\Gamma |\theta_0|}{\tau_1}\right) \right\} \quad (1)$$

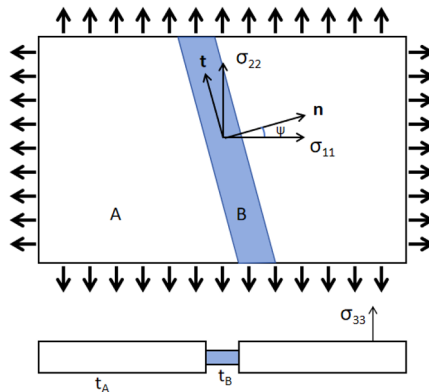
where  $\Gamma$  is accumulated shear strain inside grains, and  $\tau_0, \tau_1, \theta_0$  and  $\theta_1$  are material parameters

Fig. 2 displays the the Schematic of the MK model. The groove region is marked as region B with initial thickness  $t_{0B}$ , while the initial thickness of ungroove region A is  $t_{0A}$ . The initial thickness heterogeneity is defined as  $f_0 = t_{0B}/t_{0A}$ . In the VPSC-MK model, mixture boundary of velocity gradient  $\bar{L}_{ijA}$  and stress matrix  $\bar{\sigma}_{ijA}$  are used as:

$$\bar{L}_A = \bar{D}_{11A} \begin{bmatrix} 1 & \bar{L}_{12}/\bar{D}_{11A} & 0 \\ 0 & \rho & 0 \\ 0 & 0 & -(1 + \rho) \end{bmatrix} \quad (2)$$

$$\bar{\sigma}_A = \begin{bmatrix} \bar{\sigma}_{11A} & 0 & 0 \\ 0 & \bar{\sigma}_{22A} & 0 \\ 0 & 0 & \bar{\sigma}_{33A} \end{bmatrix} \quad (3)$$

Generally, MK model is based on the assumption of plane stress with  $\bar{\sigma}_{33A} = 0$ . In current study, the influence of thickness stress on FLC is studied with VPSC-MK model, where  $\bar{\sigma}_{33A}$  is substituted with a given value obtained from FEM simulations. The detailed calculation process of VPSC-MK can be referred to [8].



**Fig.2.** Schematic of the MK model with a thickness imperfection between regions A and B in the sheet

## 3 Results and discussion

### 3.1 Mechanical properties and formability

The engineering stress-strain curves under thickness 2.5 mm and 4.0 mm S700MC were shown in Fig. 3a. It can be seen that the same yield strength and uniform deformation stage

under two different thickness are detected. Two curves gradually differ at instability stage, in which a decline trend of instability is lower for 4.0 mm thickness sheet. Thus, final total elongation for 4.0 mm sheet is higher than that of the 2.5mm sheet.

The FLC of thickness 2.5 mm and 4.0 mm sheets were plotted in Fig. 3b. Clearly, the FLC for 4.0 mm sheet is located upper than that of 2.0 mm sheet, and major strain under plane strain (FLC<sub>0</sub>) increase from 0.23 at 2.5 mm to 0.28 at 4.0 mm. That is, better formability is achieved for sheet with larger thickness.

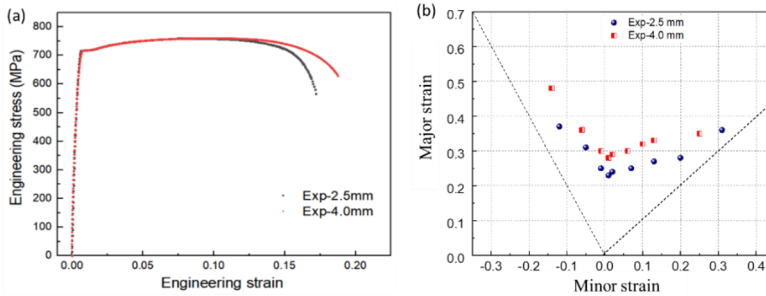


**Fig. 3.** (a) Engineering stress-strain curves and (b) FLC of 2.5 mm and 4.0 mm S700MC sheets

### 3.2 Thickness effect on tension behaviour from FEM simulation

Fig. 4 compares FEM predicted strain-stress curves with experimental ones for 2.5mm and 4.0 mm thickness with the same hardening curve. For lacking consideration of tension damage, the engineering stress-strain curves obtained by simulation show some deviation from the experimental curves in the neck region. Whereas, good agreement is observed between experimental and predicted curves at uniform section and the diffuse instability section, which verify the reliability of the FEM simulation.

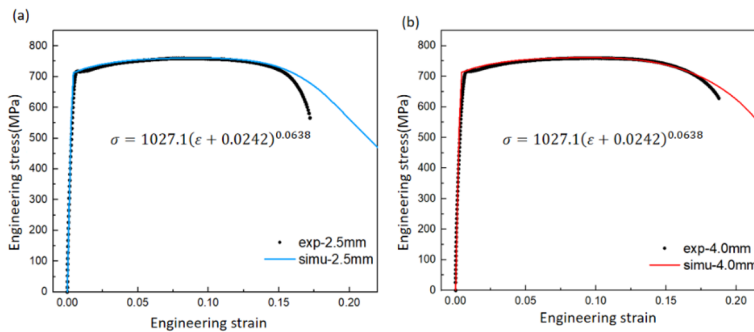


**Fig. 4.** Calibration of tensile simulation with same hardening curve: (a) 2.5 mm, (b) 4.0 mm

Fig. 5a and 5b show the strain paths of 2.5 mm and 4.0 mm thickness samples during tensile simulation. The limit strains at point 1 are (0.381, -0.175) and (0.506, -0.226) for 2.5 mm and 4.0 mm sheets, respectively. In addition, compared with the 2.5mm thickness, the limit strain at point 2 and point 3 of the 4.0 mm thickness sample are larger, indicating that more material flow to necking region under higher thickness. Seen from Fig. 5c, the thinning rate at points 1-3 is identical at the uniform region. Whereas, as compared with 2.5 mm sample, the thinning rate for 4.0 mm sample is smaller at point 1 in the necking region. Similarly, the thinning rate of 2.0 mm sample at points 2 and 3 outside the necking region is larger. Therefore, the difference in thinning rate between the inside and outside the necking area decreases with the increase of sample thickness.

Fig. 5d displays the starting points of diffusive and localized necking of 2.5 mm and 4.0 mm samples. After the diffusive instability, the principal strain increment of different thickness samples gradually differs until the localized instability point. At the same tensile displacement ( $\Delta L$ ), the difference of strain increment between point 1 and point 3 of the 4.0 mm sample is smaller than that of the 2.5 mm sample. Therefore, the strain gradient of the specimen before local necking under tension decreases with the increased thickness, which retards the occurrence of local instability and contributes to larger ultimate strain of 4.0 mm thickness specimen.

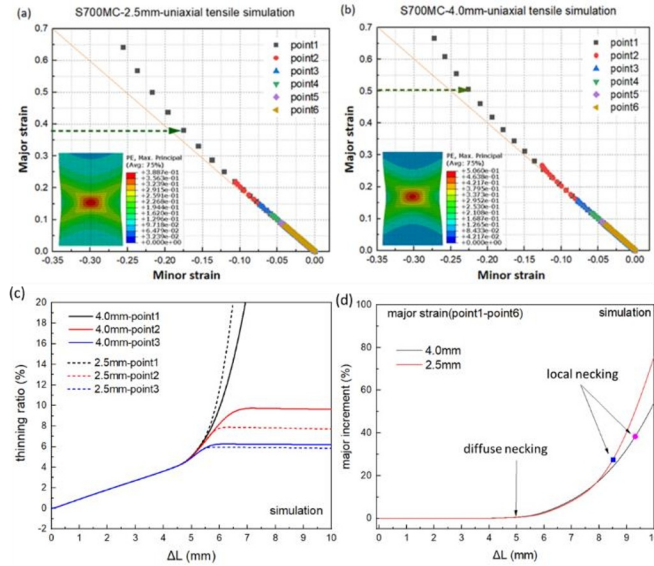


**Fig. 5.** The forming strain path of chosen nodes in FEM of (a) 2.5 mm and (b) 4.0 mm, (c) thinning ratio and (d) necking points for 2.0 and 4.0 mm samples

### 3.3 FLC prediction by VPSC-MK with thickness effect

Fig. 6a shows the equivalent stress-strain curves calculated by VPSC and the experimental curves of S700MC. The VPSC prediction using Voce hardening parameters (listed in Table 1) is of good agreement with experimental one, which can be used for VPSC-MK prediction. According to FEM simulations for different strain paths (uniaxial tension,  $\rho=-0.5$ ; plane strain tension,  $\rho=0$ ; biaxial bulge,  $\rho=1$ ), the thickness stress difference for 2.5 mm and 4.0mm samples of S700MC are given in Table 2. For VPSC-MK calculation with thickness is denoted as VPSC-MK-II. The initial thickness heterogeneity  $f_0$  was taken as 0.975, and the criterion for local necking was  $\bar{D}_{33B}/\bar{D}_{33A} \geq 20$ .

**Table 1.** Voce hardening parameters for S700MC at 298K

Modes	$\tau_0$ (MPa)	$\tau_l$ (MPa)	$\theta_0$	$\theta_l$
{110}<111>	260	121	251	10
{112}<111>	260	121	251	10

**Table 2.** Calculated thickness stress for S700MC with different thickness under typical strain paths

Thicknesses (mm)	Calculated thickness stress MPa

	$\rho=-0.5$	$\rho=0$	$\rho=1$
2.5	-43	-64	-64
4.0	-119	-124	-108

The accuracy of FLC prediction for 2.5 mm S700MC using VPSC-MK-II is significantly improved compared with that of VPSC-MK, and the absolute deviation of principal strain of  $FLC_0$  is reduced to less than 0.01. By introducing the thickness stress difference and considering the joint effect of the neck shrinkage area by the thickness compression stress difference on both sides, the predicted FLC deviation of 2.5 mm and 4.0 mm thickness of S700MC is finally controlled within 0.02.

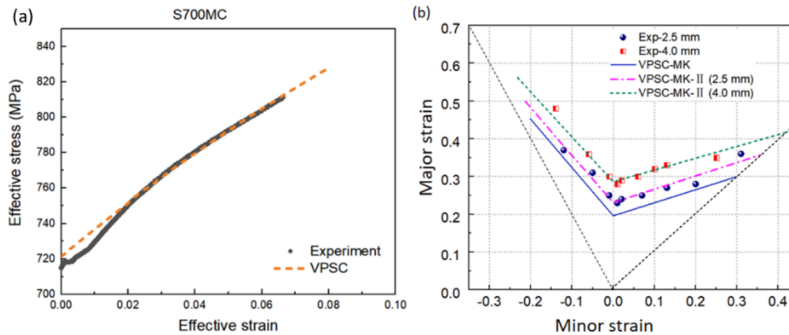


**Fig. 6.** Experimental and VPSC results of S700MC: (a) stress-strain curves; (b) FLC

## 4 Conclusions

The thickness effect mainly originates from suppressed development of local necking under higher thickness. Additionally, the established VPSC-MK model with considering varied thickness stress for different strain paths can well predict thickness-dependent FLC with error less than 5%.

## Acknowledgement

The authors would like to thank Qin-Bo Shen and Hua Zhang from Baosteel Research Institute for their help with the experimental phase of this work.

## References

1. G. Jha, S. Das, A. Lodh, A. Haldar, *Mater. Sci. Eng. A* **552**, 457-463(2012).
2. W.J. Chen, H.W. Song, L. Lazarescu, Y. Xu, S.H. Zhang, D. Banabic, *Int. J. Adv. Manuf. Technol.* **110**, 1563-1573(2020).
3. S. Panich, F. Barlat, V. Uthaisangsuk, S. Suranuntchai; S. Jirathearanat, *Mater. Des.* **51**, 756-766(2013).
4. A. Assempou, H.K. Nejadkhaki, R. Hashemi, *Comp. Mater. Sci.* **3**(48) 504-508(2010).
5. F.F. Zhang, J.S. Chen, J. Chen, *Int. J. Mech. Sci.* **89**, 92-100(2014).
6. B.L. Ma, M. Wan, H. Zhang, X.L. Gong, X.D. Wu, *J. Manuf. Processes*, **33**, 175-183(2018).
7. Y.B. Wang, C.S. Zhang, Y. Yang, S.M. Fan, G.C. Wang, G.Q. Zhao, L. Chen, *Int. J. Plast.*, **120**, 147-163(2019).
8. C. Schwindt, F. Schlosser, M.A. Bertinetti, *Int. J. Plast.* **73**, 62-99(2015).